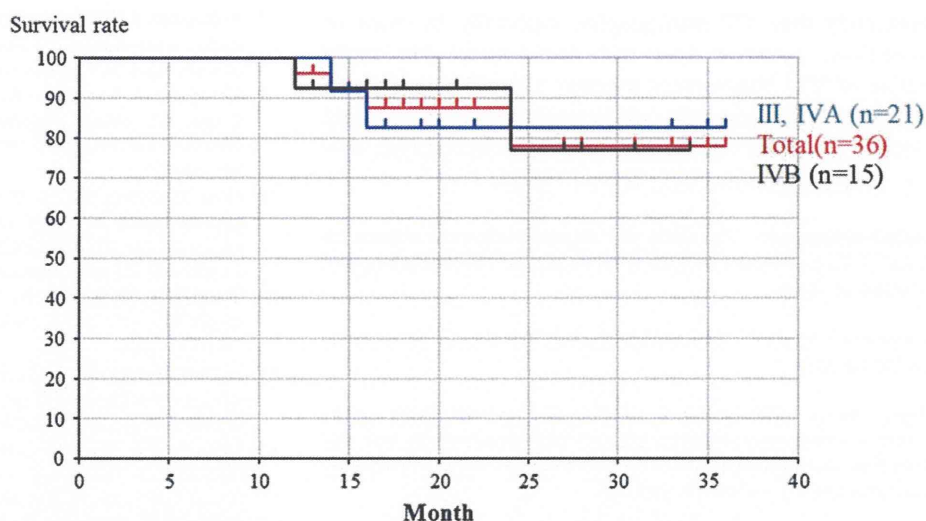


Fig. 5 The overall survival rates

alteration of the blood flow and the area supplied by the contralateral facial, or lingual artery was sufficiently confirmed to be covered by using the ICG fluorescence technique. In the present study, we sometimes perform the I-A infusion chemotherapy with manual compression of the ipsilateral facial artery in cases of advanced paranasal sinus cancers with tumors spreading to the oral cavity or facial skin. This enables alteration of the blood flow and the area supplied by the ipsilateral facial artery is sufficiently identified to be covered by using the ICG fluorescence technique. The changes of the blood flow were directly observed using the ICG fluorescence technique and effective I-A chemotherapy for the affected side alone could be conducted safely. No complication resulted from compression of the carotid artery, or facial artery. However, the same manual compression procedures during CT angiography would involve too high a radiation exposure if conducted each time. In this paper, we emphasize the following points concerning oral cancers: the drug delivery to the whole tumor crossing the midline from the contralateral side was confirmed directly by using the ICG fluorescence technique (horizontal communication). This is because there are communicating branches to the lateral sides in oral cancer. However, in the present advanced paranasal sinus cancers, communicating branches develop vertically, such as the maxillary artery communicating to branches of the facial artery (vertical communication). As a result, the significance of this method differs significantly between advanced oral cancer and advanced paranasal sinus cancer. Because one of most problematic issues of using I-A chemotherapy for advanced paranasal sinus cancers is that the tumors are often supplied by the internal carotid artery and consequently, to prevent brain complications, I-A chemotherapies were previously not indicated for such cases.

Recently, the use of ICG fluorescent image has enabled us to clearly detect tumor staining and reveal communicating branches between the internal carotid artery and maxillary artery, facial artery, and transverse facial artery (vertical communication). As a result, this ICG fluorescence imaging procedure, when combined with the technique for altering the blood flow, has enabled us to safely treat advanced paranasal sinus cancer, while improving the prognosis and preserving organ and function.

Additionally, ICG fluorescence is a useful method for confirming the arterial blood supply to paranasal sinus cancers because of the high excitation of ICG and deep penetration of the tissue to approximately 10 mm. As a result, we can use superselective I-A chemotherapy effectively for most paranasal sinus cancers that have invaded less than 10 mm. However, tumors invading more deeply than 10 mm require other imaging methods, such as simultaneous MRI angiography. Once the stained field of each feeding artery has been detected in cases of tumors invading the base of the skull or face by CT angiography, the ICG fluorescence technique can be used to compensate for defects in the CT angiography by identifying the feeding artery precisely and safely. It should be noted that a fine and sensitive endoscope for ICG fluorescence imaging is required for the detection of nasal cavity cancer. This technique is feasible and gives new promising options for advanced paranasal sinus cancers. Further investigations can lead to the development of a new minimally invasive multimodal therapy targeting advanced paranasal sinus cancers in the near future.

Conclusion

ICG fluorescence imaging for intra-arterial chemotherapy revealed the blood supplies to paranasal sinus cancers more

accurately than CT angiography, especially in cases of superficial spread or those with dental metal. The application of ICG fluorescence together with CT angiography provides more accurate information about the feeding arteries to tumors and enables effective intra-arterial chemotherapy, while avoiding complications.

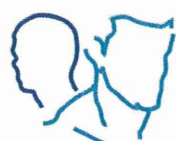
Acknowledgments This study was supported in part by a Grant for Clinical Cancer Research from the Ministry of Health, Labor, and Welfare of Japan.

Conflict of interest The authors declare that they have no competing interests.

Open Access This article is distributed under the terms of the Creative Commons Attribution License which permits any use, distribution, and reproduction in any medium, provided the original author(s) and the source are credited.

References

- Kaketa S, Korogi Y, Miyaguni Y et al (2007) A cone-beam volume CT using a 3D angiography system with a flat panel detector of direct conversion type: usefulness for superselective intra-arterial chemotherapy for head and neck tumors. *AJNR Am J Neuroradiol* 28:1783–1788
- Korogi Y, Hirai T, Nishimura R et al (1995) Superselective intraarterial infusion of cisplatin for squamous cell carcinoma of the mouth: preliminary clinical experience. *AJR Am J Roentgenol* 165:1269–1272
- Yokoyama J, Ito S, Ohba S, Fujimaki M, Ikeda K (2011) A novel approach to translymphatic chemotherapy targeting sentinel lymph nodes of patients with oral cancer using intra-arterial chemotherapy—preliminary study. *Head Neck Oncol* 3:42
- Yokoyama J, Shiga K, Saijo S et al (1999) Superselective intra-arterial infusion chemotherapy of high-dose cisplatin for advanced paranasal sinus carcinomas. *Gan To Kagaku Ryoho* 26:967–973 Japanese
- Bertino G, Benazzo M, Gatti P et al (2007) Curative and organ-preserving treatment with intra-arterial carboplatin induction followed by surgery and/or radiotherapy for advanced head and neck cancer: single-center five-year results. *BMC Cancer* 7:62
- Yokoyama J (2002) Present role and future prospect of superselective intra-arterial infusion chemotherapy for head and neck cancer. *Gan To Kagaku Ryoho* 29:169–175
- Yokoyama J (2002) Usefulness of CT-angiography for superselective intra-arterial chemotherapy for advanced head and neck cancers. *Gan To Kagaku Ryoho* 29:2302–2306
- Miyayama S, Yamashiro M, Hattori Y et al (2002) Usefulness of C-arm CT during superselective infusion chemotherapy for advanced head and neck carcinoma. *J Méd Imaging Radiat Oncol* 55:368–372
- Hirai T, Korogi Y, Ono K et al (2001) Intra-arterial chemotherapy for locally advanced and/or recurrent hepatic tumors: evaluation of the feeding artery with an interventional CT system. *Cardiovasc Intervent Radiol* 24:176–179
- Tomura N, Hashimoto M, Sashi R et al (1996) Superselective angio-CT of brain tumors. *AJNR Am J Neuroradiol* 17:1073–1080
- Hirai T, Korogi Y, Ono K, Uemura S, Yamashita Y (2004) Preoperative embolization for meningeal tumors: evaluation of vascular supply with angio-CT. *AJNR Am J Neuroradiol* 25:74–76
- Litvack ZN, Zada G, Laws ER Jr (2012) Indocyanine green fluorescence endoscopy for visual differentiation of pituitary tumor from surrounding structures. *J Neurosurg* 116:935–941
- Shimada Y, Okumura T, Nagata T et al (2011) Usefulness of blood supply visualization by indocyanine green fluorescence during esophagectomy. *Esophagus* 8:259–266
- Murakami K, Endo T, Tominaga T (2012) An analysis of flow dynamics in cerebral cavernous malformation and orbital cavernous angioma using indocyanine green videoangiography. *Acta Neurochir Online First*TM
- Fujisawa Y, Nakamura Y, Kawachi Y et al (2012) Indocyanine green fluorescence-navigated sentinel node biopsy showed higher sensitivity than the radioisotope or blue dye method, which may help to reduce false-negative cases in skin cancer. *J Surg Oncol* 106:41–45
- Ohba S, Yokoyama J, Fujimaki M et al (2012) Significant improvement in superselective intra-arterial chemotherapy for oral cancer by using indocyanine green fluorescence. *Oral Oncol* 48:1101–1105
- Yokoyama J, Ohba S, Ito S et al (2012) A feasibility study of lymphatic chemotherapy targeting sentinel lymph nodes of patients with tongue cancer (T3, N0, M0) using intra-arterial chemotherapy. *Head Neck Oncol* 4:59
- Aoki T, Yasuda D, Shimizu Y et al (2008) Image-guided liver mapping using fluorescence navigation system with indocyanine green for anatomical hepatic resection. *World J Surg* 32:1763–1767
- Yokoyama J, Fujimaki M, Ohba S et al (2013) A feasibility study of NIR fluorescent image-guided surgery in head and neck cancer based on the assessment of optimum surgical time as revealed through dynamic imaging. *Onco Targets Ther* 6:1–6



Minimally invasive procedure for reconstruction through grafting free fat placed in sternocleidomastoid muscle flap following total parotidectomy with parapharyngeal space dissection

J Yokoyama^{1*†}, S Ohba^{1†}, M Fujimaki¹, S Ito¹, M Kojima¹, T Anzai¹, R Yoshii¹, K Ikeda¹

Abstract

Background

Long periods of surgery can cause surgical complications and burnout syndrome.

Methods

Patients with parotid cancers invading the parapharyngeal space underwent total parotidectomy with parapharyngeal space dissection. Fat was harvested from the abdomen and cut into approximately 5 mm pieces. Stripped fat was inserted into the well-vascularized sternocleidomastoid (SCM) muscle. The combined free fat and SCM muscle were placed into large dead spaces resulting from the resection.

Results

Compared with fat volume at 1 month after grafting, fat preservation rates at 3, 6 and 12 months were 92%, 85% and 81%, respectively. The mean time required to harvest abdominal fat and to elevate the SCM muscle flap was 13.3 minutes and 17.2 minutes, respectively.

Conclusions

The free fat grafts in the SCM muscle flap restored facial contour and were preserved over a long period. This minimally invasive procedure is safe and can be easily performed.

Introduction

It is important to restore loss of facial contour and to prevent various surgical complications resulting from total

parotidectomy with parapharyngeal space dissection. It is standard to use microscopic surgery in the reconstruction of free flaps to be applied for reconstruction. When compared with our free fat grafting procedure, however, the standard approach demands extensive operating time and a large donor site, which requires a skin graft for resurfacing¹. In order to perform a minimally invasive surgery and to shorten the duration of surgical time, several authors have tried to use free fat grafts from the thigh or abdomen for cosmetic repair of the parotidectomy defect². However, there were significant problems resulting from the reduction of grafted fat volume. To prevent reduction in grafted fat volume, Guerrerosantos et al.³ demonstrated in an experimental study that the long-term viability of the autotransplanted fat depends on well-vascularized muscle and small fat strips. Based on this basic evidence, our new procedure combines free fat with well-vascularized sternocleidomastoid (SCM) muscle flap. The procedure is applied for reconstruction in the total parotidectomy with parapharyngeal dissection in order to accomplish a minimally invasive surgery and cosmetic reconstruction over an extended period of time.

In addition, human adipose tissue has the highest percentage of adult stem cells in the body, with as many as 5000 adipose-derived stem cells per gram of fat⁴. In this study, we have demonstrated both the current best treatment and the potential for regenerative medicine with positive implication for reconstruction when treating head and neck cancer. The

aim of this study was to determine the safety and efficiency of grafting free fat in reconstruction with regard to cosmetic consideration and preservation rate of grafting fat volume. In addition, questionnaires following total parotidectomy were used to determine patient satisfaction.

Methods and materials

The study was performed between September 2008 and June 2012 on 15 parotid cancers that invaded the parapharyngeal space. The mean age was 61.3 years (range, 30–76 years). Six patients (40%) were males and 9 (60%) were females. Ten cases (67%) were fresh cases, and five (33%) were recurrent cases. Pathological types of parotid cancers were as follows: six cases of carcinoma ex-pleomorphic adenoma, three cases of salivary duct carcinoma, two cases of mucoepidermoid carcinoma, two cases of epithelial-myoepithelial carcinoma and two cases of adenocarcinoma. The number of stage III, IVA and IVB were 2, 10 and 3, respectively (Table 1).

Surgical procedure

All patients underwent total parotidectomy with neck dissection and parapharyngeal dissection.

Total parotidectomy with parapharyngeal dissection was performed using an endoscope.

Free fat was harvested through a periumbilical incision along the inferior half of the umbilicus, extending from the 3 o'clock to the 9 o'clock position (Figure 1). Skin flaps were elevated inferiorly and laterally using curved Mayo scissors. Allis clamps were then placed on the underlying fat, which was then resected en bloc.

*Corresponding author

[†]These authors contributed equally to this work.
Email: jyokoya@juntendo.ac.jp

¹Department of Otorhinolaryngology—Head and Neck Surgery, Juntendo University School of Medicine, Tokyo, Japan


Table 1 Patient and clinical characteristics

Characteristics	Number	Characteristics	Number
Gender		Fat harvesting time	
Male	6	Range	10 min–17 min
Female	9	Mean	13 min 20 seconds
Age		Elevation of SCM muscle flap	
Range	30–76	Range	13 min–23 min
Mean	61.3	Mean	17 min 10 seconds
Median	67	Lenth of SCM muscle flap	
Previous treatment		Range	8.5 cm–10.8 cm
Untreated	10	Mean	9.3 cm
Recurrent	5	Total volume of drainage after surgery	
Stage		Neck	
III	2	Range	11–242 ml
IVA	10	Mean	67 ml
IVB	3	Donor site	
Pathological type		Range	4–28 ml
Carcinoma expleomorphic adenoma	6	Mean	12 ml
Salivary duct carcinoma	3	Drain indwelling periods	
Mucoepidermoid carcinoma	2	Neck	
Epithlial-myoepithlial carcinoma	2	Range	1–6 days
Adenocarcinoma	2	Mean	2.5 days
		Donor site	
		Range	1–2 days
		Mean	1.07 days
		Questionnaire data	
		Mean facial contour deformity	1.33
		Mean incisional scare	1.06

The fat was cut off the anterior rectus fascia and delivered through the periumbilical incision. The harvested fats was rinsed in saline, and then cut to around 5mm. These stripped fats were

washed with sterilized saline and then inserted into the well-vascularized SCM muscle flap. The combined free fat and SCM muscle flap were placed into large dead spaces which resulted

from the resection of the parotid cancer. As a result, the facial nerve was covered with the combined flap and facial contour could be restored (Figure 2). A 10-Fr closed suction drain was used in all cases to drain both the parotid and abdominal incisions. Drains were removed when output was less than 15 mL in a 24-hour period. The grafted fat was observed at 1, 3, 6 and 12 months after grafting through magnetic resonance imaging (MRI). We calculated the percentage of fat volume 1 month later, and used this as the baseline for comparative analysis at 3, 6 and 12 months after fat grafting (Figure 3).

We also evaluated patient satisfaction by using a modified Taylor SM's questionnaire⁵ at 6 months, postoperatively. Items included patient perception of facial symmetry, incisional scar and symptoms of Frey's syndrome. Patients were asked to grade their level of satisfaction on a 10-point Likert scale, whereby a score of 1 indicated complete satisfaction and a score of 10 indicated complete dissatisfaction (Table 2).

Results

All patients underwent total parotidectomy with ipsilateral neck dissection (levels I–IV) and parapharyngeal dissection. In addition, facial nerve resection and reconstruction were performed in 4 out of 15 cases. Skull base surgery requiring the resection of involved cranial dura and reconstruction were performed in 3 out of 15 cases.

Through MRI, the viability of the grafting fat placed in the SCM flap was demonstrated to be vital and active. Figure 3 demonstrated the change of grafted fat volume from 1 month to 12 months in a recurrent parotid cancer.

MRI also showed that fat preservation rates at 3, 6 and 12 months were 92%, 85% and 81%, respectively (Figure 4). In addition, MRI showed that the viability of the grafting fat

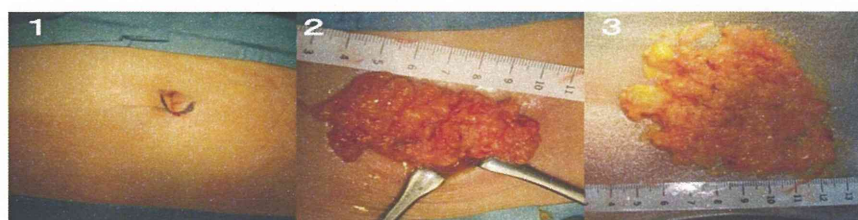


Figure 1: The fat harvesting procedure through a periumbilical incision. (1) A periumbilical incision along the inferior half of the umbilicus. (2) Harvested free fat through a periumbilical incision. (3) The harvested fats were cut to around 5 mm.

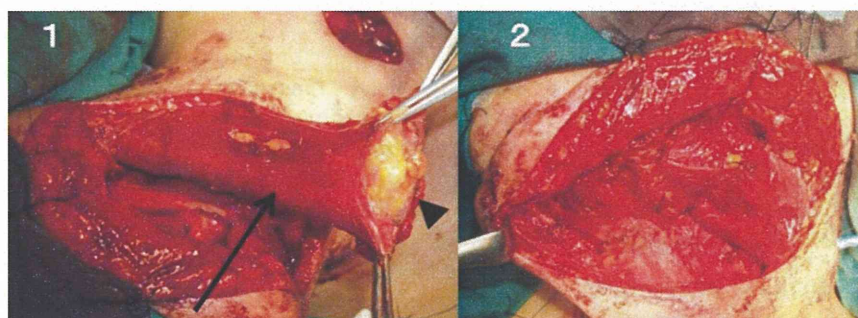


Figure 2: The combined free fat and SCM muscle flap. (1) The elevated SCM muscle flap. The muscle flap maintains blood supply by the superficial transverse cervical artery. This novel flap has a wide range and well-vascularized muscle flap. Arrow: the sternum head for the muscle flap. Arrow head: stripped free fat. (2) Reconstruction of defects following resection of parotid cancer by the combined well-vascularized SCM muscle flap and free abdominal fat.

placed in the SCM flap remained vital over the 12-month monitoring period (Figure 5).

The mean time required to harvest abdominal fat was 13 minutes and 20 seconds. In addition, it required a mean time of 17 minutes and 10 seconds to elevate the SCM muscle flap (Table 1). The procedure is safe and can be easily accomplished with a minimally invasive method. Complications are rare and easily managed.

Drains were removed when the total output was less than 15 mL in a 24-hour period. The mean period of drains indwelling in the neck and the donor site was 2.5 days and 1.1 days, respectively. The mean total suction volume through drains after surgery of the neck and the donor site were 67 mL (11–242 mL) and 12 mL (4–28 mL), respectively (Table 1).

Complications

There were no major complications such as postoperative bleeding, seromas or fat liquefaction. However, one patient required oral antibiotics for a minor infection.

Six patients out of all patients underwent postoperative chemoradiotherapy. However, no patients experienced grafted fat necrosis or severe reduction of grafted fat compared with patients with non-receiving postoperative chemoradiotherapy.

The questionnaire data showed that the mean score regarding the facial contour deformity and incisional scar was 1.33 and 1.06, respectively. All patients treated by this method demonstrated high satisfaction in their perceptions of facial contour and incisional scars at 6 months (Table 1).

The questionnaire also indicated that no patient experienced subjective symptoms of Frey's syndrome or facial flushing at the site of surgery. Donor site morbidity was of no concern to the patients.

The combined free fat and SCM muscle flap are especially useful following total parotidectomy with parapharyngeal space tumour resection.

Discussion

Total parotidectomy with parapharyngeal space dissection causes significant loss of facial contour and various surgical complications. To prevent significant complications, free flaps are usually applied for reconstruction. However, free flaps are associated with much greater operative time and a large donor site, which requires a skin graft for resurfacing¹. Consequently, elder or comorbid patients could sometimes experience severe stress as a result of surgery. In order to perform a minimally invasive surgery and to shorten the duration of the surgical time, several researchers have tried to use free fat grafts from the thigh or abdomen for cosmetic repair of the parotidectomy defect². Dermal fat is believed that its attached vasculature to fat can aid in revascularization of the grafted fat. However, the procedure of harvesting dermal fat requires moderately-high level technique and additional time. Furthermore, limiting size or reduction of volume are significant problems^{3,5,6}. To prevent these problems, application of autologous platelet adhesive to defect of superficial parotidectomy is reported to improve outcomes⁷. However, there have been controversial experimental reports⁸, and reconstruction using the free fat grafts has not been conclusively established.

In an experimental study, Guerrosantos et al.³ indicated that the long-term viability of the autotransplanted fat depends on well-vascularized muscle and small fat strips. However, only small strips fat cannot

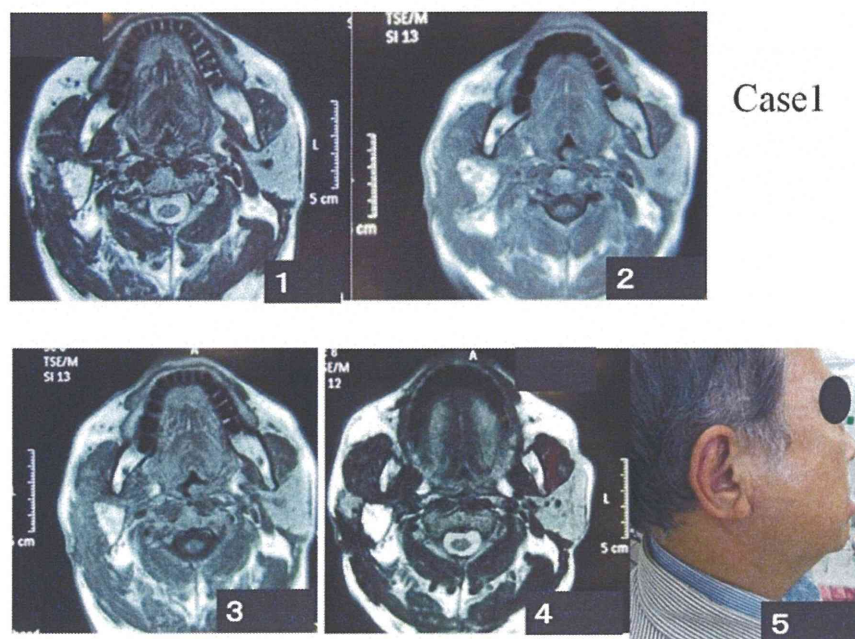


Figure 3: The change of grafted fat volume through MRI in recurrent parotid cancer. Case 1: recurrent parotid cancer. MRI (postoperative 1 month to 12 months) 1: postoperative 1 month, 2: postoperative 3 month, 3: postoperative 6 month, 4: postoperative 12 month, 5: patient's profile in postoperative 12 months.

Grafted fat preservation rate (compared with postoperative 1 month)

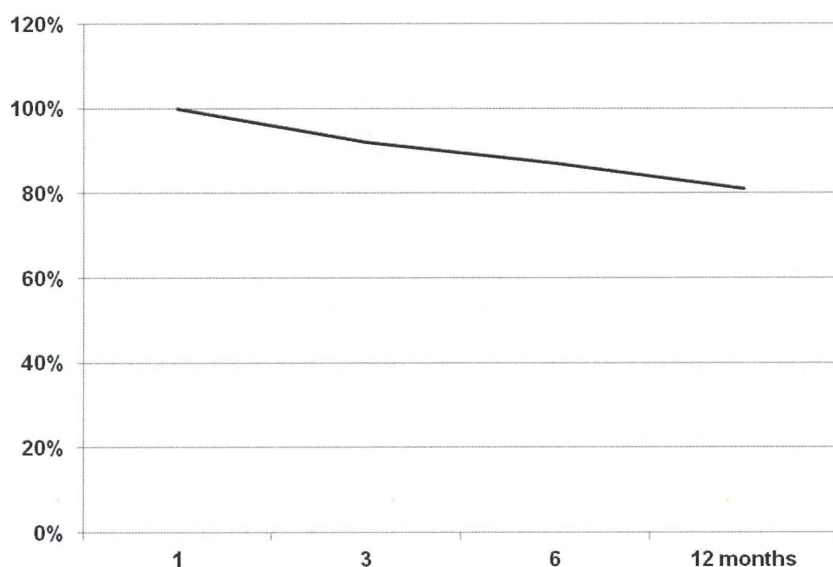


Figure 4: The grafted fat preservation rate (compared with postoperative 1 month).

effectively retain good facial contour due to soft and easy scatter. This results in significant deformity and an incisional scar. In addition, small strips of fat are sucked easily into drainage tubes and often obstruct them. To resolve these problems, small fat strips need to be wrapped by well-vascularized muscle flap.

However, in case of parotid cancer, all cases were performed at the same time as neck dissection (levels I–IV) of the ipsilateral side. SCM has three main feeding arteries including occipital artery, superior thyroid artery and superficial transverse cervical artery. Both feeding arteries of the occipital artery and the superior thyroid artery are usually cut to perform neck dissection in order to control neck metastasis. To elevate upper pedicle SCM muscle flap, both heads of clavicle and sternum of SCM are cut and the upper pedicle SCM muscle flap usually result in an ischaemic flap. Based on the three main feeding arteries for SCM, we investigated only the sternum head for muscle flap while maintaining blood supply by the superficial transverse cervical artery derived from the subclavicular artery. This novel procedure has wide range and well-vascularized muscle flap. The current study combined well-vascularized SCM muscle flap and free abdominal fat to reconstruct defects following resection of head and neck cancers.

The use of dermis-fat grafts from the thigh or abdomen for the parotidectomy defect has been reported to be useful for cosmetic repair^{9,10}. The main indications for this method were benign parotid tumour and small superficial parotidectomy^{2,9,10}. However, approximately 30% of the fat graft is resorbed; fat graft reconstruction should not be used in patients with malignant tumours due to the concern that the graft may mask recurrence and adhere to the cancer⁹. We developed a procedure to wrap free fats with the SCM muscle flap and graft to the defect of

Competing interests: none declared. Conflict of interests: none declared.
All authors contributed to conception and design, manuscript preparation, read and approved the final manuscript.
All authors abide by the Association for Medical Ethics (AME) ethical rules of disclosure.

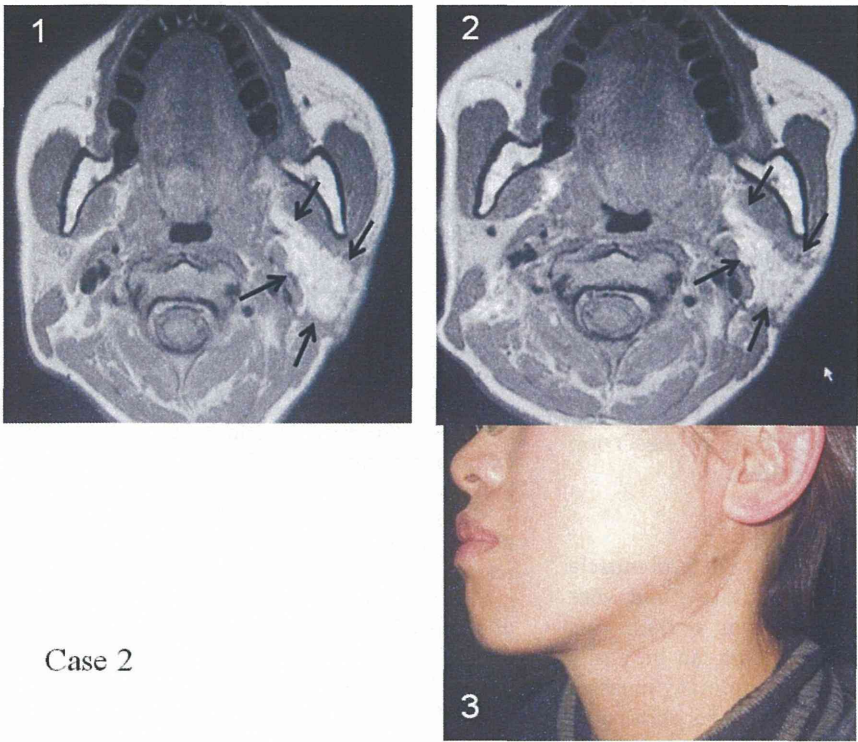
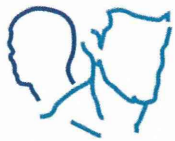


Figure 5: Case 2: recurrent parotid cancer. (1) MRI (postoperative 1 month). (2) MRI (postoperative 12 months). (3) Patient's profile (postoperative 12 months).

parotidectomy. As a result, free fats cannot contact the cancer directly as they are separated by the SCM muscle flap. Our report is the first investigation of grafted free fats that demonstrate effectiveness and safety for large defects following resection of advanced parotid cancers and neck and parapharyngeal dissection. In addition, patients with advanced parotid cancer sometimes receive postoperative radiation treatment. In the current study, six (40%) patients received postoperative chemoradiotherapy. All of these patients tolerated postoperative chemoradiotherapy and grafted fat necrosis, or significant reduction of grafted fat did not result from postoperative chemoradiotherapy. As a result, our novel procedure combined with well-vascularized SCM muscle flap and free abdominal fat can contribute to reconstruction of defects resulting from head and neck cancers. Recently, human adipose tissue has been reported to have the highest

Table 2 Patient satisfaction after parotidectomy with fat graft reconstruction
Questionnaire: Please complete the following questions to the best of your ability. Ensure that the responses reflect <input type="checkbox"/> your own opinion. Should you have any questions, please do not hesitate to ask your surgeon or a clinic nurse for assistance. Thank you for contributing to our study.
1. How would you rate the facial contour deformity following your operation? (please circle) <input type="checkbox"/> <input type="checkbox"/> <input type="checkbox"/> No deformity 1 2 3 4 5 6 7 8 9 10 Worst deformity
2. Please rate your incisional scar by circling the number below. <input type="checkbox"/> <input type="checkbox"/> <input type="checkbox"/> No scar 1 2 3 4 5 6 7 8 9 10 Worst scar
3. Do you experience facial sweating at the site of your operation when you eat? (please circle) <input type="checkbox"/> <input type="checkbox"/> <input type="checkbox"/> <input type="checkbox"/> YES <input type="checkbox"/> NO
4. Do you experience facial flushing at the site of your previous surgery with eating? (please circle) <input type="checkbox"/> <input type="checkbox"/> <input type="checkbox"/> <input type="checkbox"/> YES <input type="checkbox"/> NO
5. Would you undergo another operation to correct your facial contour deformity? (please circle) <input type="checkbox"/> <input type="checkbox"/> <input type="checkbox"/> <input type="checkbox"/> YES <input type="checkbox"/> NO
6. Would you undergo treatment for your incisional scar? <input type="checkbox"/> <input type="checkbox"/> <input type="checkbox"/> <input type="checkbox"/> YES <input type="checkbox"/> NO
7. Would you undergo treatment for your facial sweating or facial flushing? <input type="checkbox"/> <input type="checkbox"/> <input type="checkbox"/> <input type="checkbox"/> YES <input type="checkbox"/> NO
8. How much of a problem is your fat graft donor site? (please circle) Not a problem at all 1 2 3 4 5 6 7 8 9 10 Extremely problematic

Licensee OA Publishing London 2013. Creative Commons Attribution License (CC-BY)

FOR CITATION PURPOSES: Yokoyama J, Ohba S, Fujimaki M, Ito S, Kojima M, Anzai T, Yoshii R, Ikeda K. Minimally invasive procedure for reconstruction through grafting free fat placed in sternocleidomastoid muscle flap following total parotidectomy with parapharyngeal space dissection. Head Neck Oncol. 2013 Apr 01;5(4):42.

Competing interests: none declared. Conflict of interests: none declared.
All authors contributed to conception and design, manuscript preparation, read and approved the final manuscript.
All authors abide by the Association for Medical Ethics (AME) ethical rules of disclosure.



percentage of adult stem cells in the body, with as many as 5000 adipose-derived stem cells per gram of fat⁴. In particular, human subcutaneous adipose tissue is an abundant and accessible source of multipotent adult stem cells^{11,12}. Considering the high preservation rate of grafted free fats, we believe that our small striped free fats can be supplied with blood by well-vascularized muscle flap. In addition, the grafted free fats include abundant and accessible source of multipotent adult stem cells. As a result, fragile lipid-filled adipocytes are more easily damaged and preadipocytes can survive without nutrition for much longer than adipocytes and have a much lower oxygen consumption rate. In our case, preadipocytes and adipose-derived stem cells may be selectively grown and may truly indicate the only tissue to survive transplantation.

Regenerative medicine by using stem cells is developing in basic science in order to determine ideal treatments. However, at this time, it is difficult to perform regenerative medicine for clinical application using stem cells derived from fat. However, our method of using abdominal fat grafts including abundant stem cells can be easily performed, with safety and reliability. Abdominal fat includes rich stem cells that can regenerate fat, resulting in the preservation of free grafted fat volume over a long period of time. These data can draw attention to new regenerative medicine in the future.

Based on this basic evidence, our new combined procedure of free fat and well-vascularized SCM muscle flap were applied for reconstruction for total parotidectomy with parapharyngeal dissection in order to accomplish a minimally invasive surgery and cosmetic reconstruction over a long duration.

The questionnaire indicated that no patient experienced subjective

symptoms of Frey's syndrome or facial flushing at the site of surgery. Donor site morbidity was no concern to the patients. All patients treated by this method demonstrated high satisfaction in their perceptions of facial contour and incisional scars at 6 months. However, the SCM muscle flap could not always prevent subjective symptoms of Frey's syndrome or facial flushing at the site of surgery¹³. As a result, our combined free fat and SCM muscle flap were especially useful following total parotidectomy with parapharyngeal dissection without complications.

Conclusions

The free fat grafts in the SCM muscle flap restored facial contour and were preserved over a long period. This procedure is safe and can be easily performed. It is a minimally invasive procedure which can be performed without complications.

Acknowledgment

This study was supported in part by a Grant for Clinical Cancer Research from the Ministry of Health, Labor and Welfare of Japan.

Authors' contributions

MF, SI and MK conceived the study and participated in its design and coordination. JY, TA and RY drafted the manuscript. JY and KI were involved in revising the manuscript.

References

1. Teknos TN, Nussenbaum B, Bradford CR, Prince ME, ElKashlan H, Chepeha DB. Reconstruction of complex parotidectomy defects using the lateral arm free tissue transfer. *Otolaryngol Head Neck Surg*. 2003 Sep;129(3):183–91.
2. Harada T, Inoue T, Harashina T, Hatoko M, Ueda K. Dermis fat graft after parotidectomy to prevent Frey's syndrome and the concave deformity. *Ann Plast Surg*. 1993 Nov;31(5):450–2.
3. Guerrero Santos J, Gonzalez-Mendoza A, Masmela Y, Gonzalez MA, Deos M, Diaz

- P. Long-term survival of free fat grafts in muscle: an experimental study in rats. *Aesthetic Plast Surg*. 1996 Sep;20(5):403–8.
4. Strem BM, Hicok KC, Zhu M, Wulur I, Alfonso Z, Schreiber RE, et al. Multipotential differentiation of adipose tissue-derived stem cells. *Keio J Med*. 2005 Sep;54(3):132–41.
5. Taylor SM, Yoo J. Prospective cohort study comparing subcutaneous and sub-superficial musculoaponeurotic system flaps in superficial parotidectomy. *J Otolaryngol*. 2003 Apr;32(2):71–6.
6. Conger BT, Gourin CG. Free abdominal fat transfer for reconstruction of the total parotidectomy defect. *Laryngoscope*. 2008 Jul;118(7):1186–90.
7. Chandarana S, Fung K, Franklin JH, Kotylak T, Matic DB, Yoo J. Effect of autologous platelet adhesives on dermal fat graft resorption following reconstruction of a superficial parotidectomy defect: a double-blinded prospective trial. *Head Neck*. 2009 Apr;31(4):521–30.
8. Por YC, Yeow VK, Louri N, Lim TK, Kee I, Song IC. □ Platelet-rich plasma has no effect on increasing free fat graft survival in the nude mouse. *J Plast Reconstr Aesthet Surg*. 2009 Aug;62(8):1030–4.
9. Curry JM, Fisher KW, Heffelfinger RN, Rosen MR, Keane WM, Pribitkin EA. Superficial musculoaponeurotic system elevation and fat graft reconstruction after superficial parotidectomy. *Laryngoscope*. 2008 Feb;118(2):210–5.
10. Davis RE, Guida RA, Cook TA. Autologous free dermal fat □ graft: reconstruction of facial contour defects. *Arch Otolaryngol Head Neck Surg*. 1995 Jan;121(1):95–100.
11. Gimble JM, Katz AJ, Bunnell BA. Adipose-derived stem cells for regenerative medicine. *Circ Res*. 2007 May;100(9):1249–60.
12. Barrilleaux B, Phinney DG, Prockop DJ, O'Connor KC. Review: ex vivo engineering of living tissues with adult stem cells. *Tissue Eng*. 2006 Nov;12(11):3007–19.
13. Sanabria A, Kowalski LP, Bradley PJ, Hartl DM, Bradford CR, de Bree R, et al. Sternocleidomastoid muscle flap in preventing Frey's syndrome after parotidectomy: a systematic review. *Head Neck*. 2012 Apr;34(4):589–98.

Licensee OA Publishing London 2013. Creative Commons Attribution License (CC-BY)

FOR CITATION PURPOSES: Yokoyama J, Ohba S, Fujimaki M, Ito S, Kojima M, Anzai T, Yoshii R, Ikeda K. Minimally invasive procedure for reconstruction through grafting free fat placed in sternocleidomastoid muscle flap following total parotidectomy with parapharyngeal space dissection. *Head Neck Oncol*. 2013 Apr 01;5(4):42.

Tumor-targeted chemotherapy with the nanopolymer-based drug NC-6004 for oral squamous cell carcinoma

Kazuhira Endo,¹ Takayoshi Ueno,¹ Satoru Kondo,¹ Naohiro Wakisaka,¹ Shigeyuki Murono,¹ Makoto Ito,¹ Kazunori Kataoka,^{2,3} Yasuki Kato⁴ and Tomokazu Yoshizaki^{1,5}

¹Division of Otolaryngology, Graduate School of Medical Science, Kanazawa University, Ishikawa; ²Department of Materials Engineering, Graduate School of Engineering, The University of Tokyo, Tokyo; ³Division of Clinical Biotechnology, Center for Disease Biology and Integrative Medicine, Graduate School of Medicine, The University of Tokyo, Tokyo; ⁴Research Division, NanoCarrier Co., Ltd, Chiba, Japan

(Received October 30, 2012/Revised November 22, 2012/Accepted December 2, 2012/Accepted manuscript online December 6, 2012/Article first published online January 30, 2013)

Cisplatin (CDDP) has been a key drug for chemotherapy in patients with head and neck squamous cell carcinoma. Nephrotoxicity is one of its adverse reactions that are dose limiting. To increase its antitumor effects and reduce such toxicity problems, polymeric micelles carrying CDDP (NC-6004) have been developed. The present study was designed to evaluate the efficacy and safety of NC-6004 for oral squamous cell carcinoma. *In vitro* antitumor activity was assayed in four oral squamous cell carcinoma cell lines. To investigate the antitumor and nephrotoxic effects of NC-6004, nude mice bearing OSC-19 were administered NC-6004 or CDDP. The *in vitro* growth-inhibitory effect of NC-6004 was significantly less than that of CDDP. However, both NC-6004 and CDDP showed equivalent antitumor effects *in vivo*. Mice with CDDP developed renal cell apoptosis; however, those injected with NC-6004 were almost free of renal cell injury. Moreover, in an orthotopic tongue cancer model using OSC-19, NC-6004 reduced the rate of sentinel lymph node metastasis to lower than that with CDDP. In conclusion, considering the potential advantages in terms of noticeable antitumor activity, lymphatic drug delivery and reduced nephrotoxicity, NC-6004 represents a significant structural improvement in the development of a platinum complex. (*Cancer Sci* 2013; 104: 369–374)

Head and neck cancer remains a significant public health problem and ranks in the six leading cancers by incidence worldwide, with an estimated 600 000 new cases every year.⁽¹⁾ Cisplatin (*cis*-dichlorodiammineplatinum; CDDP) has been demonstrated to be one of the most effective cytotoxic agents⁽²⁾ and the CDDP-based chemotherapy regimen has gained widespread use in patients with head and neck squamous cell carcinoma (HNSCC). However, its administration has been hindered by its adverse reactions, for example, nephrotoxicity, neurotoxicity, gastrointestinal toxicity, hematological toxicity and ototoxicity.⁽³⁾ Among these, the significant risk of nephrotoxicity frequently hinders the use of high doses to maximize its antineoplastic effects, which might be the cause of treatment failure.

To overcome these problems and improve the therapeutic effect of CDDP, we have been applying superselective supra-dose intra-arterial CDDP infusion for advanced HNSCC.⁽⁴⁾ However, since this technique is more complicated than that of i.v. infusion of antitumor drugs, it is not prevalent in the chemotherapy scene. Recently, several kinds of nanoparticle therapeutic platforms, including liposomes, nanoparticles and polymeric micelles, have been developed based on the idea that the drug delivery system (DDS) can accumulate in the tumor selectively, with reduced distribution in normal tissues and minimized undesirable side-effects.^(5–7) NC-6004, which is

a CDDP-incorporating polymeric micellar nanoparticle, enhanced antitumor activity and reduced the nephrotoxicity and neurotoxicity of CDDP in gastric cancer.^(8–10) Poly(ethylene glycol)-poly(glutamic acid) block copolymers (PEG-P [Gu]) confer a stealth property to the formulation, which allows the micellar drug preparation to be less avidly taken up by the reticuloendothelial system and retained in the circulation for a longer period of time. This has been recognized as the enhanced permeability and retention (EPR) effect where extravasation of high-molecular-weight micelles through leaky tumor capillary fenestrations, which result from abnormalities in angiogenesis at the tumor site, lead to accumulation and retention for a long time.⁽¹¹⁾ A prolonged circulation time and the ability of EPR lead to the accumulation of CDDP in tumor tissues. NC-6004 has been previously shown to possess significant antitumor activity for human gastric cancer cells in a mouse model.⁽¹⁰⁾ However, the efficacy of NC-6004 in head and neck cancer has never been studied.

In the present study, we analyzed the cytotoxicity of NC-6004 using the MTS assay and apoptosis assay on oral squamous cell carcinoma cell lines. Antitumor and nephrotoxic effects of NC-6004 were investigated and compared with those of CDDP in *in vivo* experiments. As frequent involvement of regional lymph nodes, especially the sentinel lymph node (SLN), is one of the outstanding features of oral SCC, we further evaluated the lymphatic distribution of NC-6004 in order to develop a target therapy for cervical lymph node metastasis, which also has never been evaluated.

Materials and Methods

Materials. Human oral squamous cell carcinoma cell lines OSC-19, OSC-20, HSC-3 and HSC-4 were used for these experiments. OSC-19 and OSC-20 were maintained in Eagle's minimum essential medium supplemented with 10% fetal bovine serum. HSC-3 and HSC-4 were maintained in Dulbecco's modified Eagle's medium with 10% fetal bovine serum. Luciferase-transfected OSC-19 LN2-Luc cells were kindly provided by Dr Jeffrey N. Myers (The University of Texas MD Anderson Cancer Center, Houston, TX, USA).⁽¹²⁾ The CDDP was obtained from Nippon Kayaku Co., LTD (Tokyo, Japan). NC-6004 was supplied by NanoCarrier Co. Ltd (Chiba, Japan).⁽⁹⁾ The luciferase antibody was purchased from MBL (Nagoya, Japan). 6-week-old female BALB/c-nu/nu mice were purchased from Charles River Japan Inc. (Kanagawa, Japan). All animal procedures were performed in

⁵To whom correspondence should be addressed.
E-mail: tomoy@med.kanazawa-u.ac.jp

compliance with the guidelines for the Ethical Committee of the Laboratory for Animal Experiments, Graduate School of Medical Science, Kanazawa University.

In vitro growth-inhibition assay. Head and neck cancer cell lines were evaluated in the present study. A 3-(4,5-dimethylthiazol-2-yl)-5-(3-carboxymethoxyphenyl)-2-(4-sulfophenyl)-2H-tetrazolium salt (MTS) assay was performed to assess the effect of cell proliferation using the CellTiter 96 Aqueous One Solution Cell Proliferation Assay (Promega, WI, USA). Briefly, cells were seeded in 96-well culture plates at a density of 2×10^3 cells/well. After 24 h incubation with 0.9% NaCl (control), a graded concentration of CDDP or NC-6004 was added to each well and incubated for 48 or 72 h. Following 2 h incubation of MTS reagent, optical density was read with a Microplate Reader Manager (Molecular Device, Sunnyvale, CA, USA) at a wavelength of 490 nm. The IC_{50} values represented the drug concentrations that reduced the mean absorbance at 490 nm to 50% in the untreated control well.

Apoptosis assay. Before incubation with drugs, OSC-19 cells were cultured in serum-free medium for 24 h. Then, with a series of CDDP- or NC-6004-containing medium for 24 h, caspase-3 activity was measured using the Caspase-Glo 3/7 Assay (Promega, WI, USA) according to the manufacturer's instructions. Briefly, cells with CDDP or NC-6004 were added with Caspase-Glo 3/7 Reagent (promega) to each well of the 96-well plate. The luminescence of each sample was measured with a Typhoon9200 imager (GE Healthcare UK Ltd, Amersham, UK).

Evaluation of antitumor activity. For this experiment, 1×10^5 OSC-19 cells were injected s.c. on the dorsal skin of BALB/c-nu/nu mice. When tumor diameters reached 3 mm, tumor-bearing mice were allocated randomly to drug administration groups. There were three test groups as follows: control group; CDDP treatment; and NC-6004 treatment. Drugs were injected i.v. via the tail vein each week, with three administrations in total. Mice were administered a single i.v. injection of 5% glucose solution (control), CDDP (5 mg/kg) or NC-6004 (an equivalent dose of 5 mg/kg CDDP). The tumor volume was calculated using the formula: tumor volume (mm^3) = $a \times b$ (where a is the longest tumor diameter and b is the shortest tumor diameter).

TUNEL assay. A TUNEL assay was performed for the detection and quantitation of kidney cell apoptosis, as previously described.⁽¹³⁾ The ApoAlert DNA Fragmentation Assay Kit obtained from Clontech (La Jolla, CA, USA) was used to assess apoptosis-induced nuclear DNA fragmentation via a fluorescence assay. On day 28 after administration of the drug, the mice, in which the same experimental protocol described in "Evaluation of antitumor activity" was used, were killed. The kidney was removed and serum was collected. The kidney was fixed in 10% formalin solution. Paraffin sections were deparaffinized. TUNEL-positive apoptotic cells were detected using visualization with a fluorescent microscope. The number of apoptotic cells per 100 at five fields in the tubule cells of the kidney was counted. In each blood sample, the plasma concentrations of creatinine were measured by SRL Laboratories (Tokyo, Japan).

Assessment of cervical lymph node metastasis. BALB/c-nu/nu mice were anesthetized and 1×10^5 OSC-19 LN2-Luc cells were then injected submucosally into the right side of the tongue using a tuberculin syringe with a 30-gauge hypodermic needle.⁽¹⁴⁾ Mice were administered a sublingual injection of 5% glucose solution (control), CDDP (5 mg/kg) or NC-6004 (an equivalent dose of 5 mg/kg CDDP) each week around the implanted tumor, with three administrations in total. On day 21 after implantation of OSC-19 LN2-Luc cells, the mice were killed. Cervical lymph nodes were resected and histopathologically examined using HE staining

and luciferase staining to confirm the presence or absence of tumors. The presence of lymphatic metastasis was compared among groups.

For the pharmacokinetic study, drug concentrations were measured in cervical lymph nodes and plasma. After the injection of CDDP or NC-6004, samples were collected at 1, 24, 72 and 144 h.

Statistical analysis. Data were expressed as the mean \pm SD. Differences between test groups were analyzed using the Student's *t*-test. The spss statistical software version 18 (SPSS Japan Inc., Tokyo, Japan) was used. A value of $P < 0.05$ was considered to be significant.

Results

Sensitivity of oral cancer cells to CDDP. The cytotoxicity of NC-6004 was evaluated in comparison to that of CDDP in oral carcinoma cell lines. The IC_{50} values, calculated from dose-survival curves obtained after 48 and 72 h treatment from the MTS assay, were investigated (Table 1). The IC_{50} values for CDDP ranged from 16.5 to 28.3 μM at 48 h and 17.6 to 20.5 μM at 72 h. NC-6004 showed a growth inhibitory potency that was lower than that of CDDP, with IC_{50} values ranging from 118.9 to 398.4 μM at 48 h and 113.9 to 119.3 μM at 72 h. The growth inhibitory effect of CDDP *in vitro* was seven- to 14-fold more potent than that of NC-6004.

Upregulation of caspases by cisplatin and NC-6004. When OSC-19 cells were exposed to increasing concentrations of CDDP, caspase-3 and caspase-7 were activated in a dose-dependent manner. Neither CDDP nor NC-6004 significantly influenced caspase activity at a concentration of 0.05 $\mu g/\mu L$. However, CDDP and NC-6004 increased caspase activity at a concentration of 2.5 $\mu g/\mu L$ by approximately 142–331% and 165–170%, respectively (Fig. 1). These data indicate that both drugs induced apoptosis in a dose-dependent manner, which relied on caspase-3 and caspase-7 activation.

Antitumor activity of NC-6004 on OSC-19 xenograft. The antitumor activity of NC-6004 or CDDP was evaluated in oral carcinoma-bearing mice. All mice survived the experiment. In OSC-19 xenografts, the tumor started to grow on day 14. On day 35, mice treated with either CDDP or NC-6004 showed 4.9- or 6.6-fold tumor growth inhibition relative to the control group, respectively (Fig. 2). There were no significant differences for the growth inhibitory effect between the two groups receiving chemotherapy.

Decreased nephrotoxicity of NC-6004 to CDDP in mice. Nude mice given an injection of CDDP or NC-6004 at a dose of 10 mg/kg were used to evaluate the structural and functional consequences of CDDP-induced nephrotoxicity. In the control group, no apoptosis in the tubule cells of the kidney was detected. Drug-induced tubule cell apoptosis was recognized as TUNEL-stained cells (Fig. 3a–c). Apoptotic cells from CDDP- or NC-6004-treated mice were counted and scored as structural

Table 1. The 50% inhibitory concentration (IC_{50}) values of cisplatin (CDDP) and NC-6004 (μM)

Cell line	IC_{50}			
	48 h		72 h	
	CDDP	NC-6004	CDDP	NC-6004
OSC-19	28.3	129.3	17.6	117.0
OSC-20	22.4	398.4	18.4	113.9
HSC-3	11.2	110.5	10.2	71.7
HSC-4	16.5	118.9	20.5	119.3